

# Mobile Satellite Channel with Angle Diversity: the MiLADY Project

T. Heyn<sup>1</sup>, E. Eberlein<sup>1</sup>, D. Arndt<sup>2</sup>, A. Heuberger<sup>2</sup>, B. Matuz<sup>3</sup>, F. Lázaro Blasco<sup>3</sup>, R. Prieto-Cerdeira<sup>4</sup>, J. Rivera-Castro<sup>4</sup>

<sup>1</sup> Fraunhofer Institute for Integrated Circuits - IIS, Erlangen, Germany, {thomas.heyn, ernst.eberlein}@iis.fraunhofer.de

<sup>2</sup> Fraunhofer Institute for Integrated Circuits - IIS, Ilmenau, Germany, {daniel.arndt, albert.heuberger}@iis.fraunhofer.de

<sup>3</sup> German Aerospace Center (DLR), Oberpfaffenhofen, Germany, {Balazs.Matuz, Francisco.LazaroBlasco}@dlr.de

<sup>4</sup> European Space Agency, ESTEC, Noordwijk, The Netherlands, {Roberto.Prieto.Cerdeira, Juan.Rivera.Castro}@esa.int

**Abstract** - Future broadcasting to mobile services may consider satellite angle diversity to overcome fading propagation effects on the land mobile satellite (LMS) environment. For that reason, an experimental campaign for gathering relevant experimental data and improve angle diversity models has been carried out in the MiLADY project. Its main focus is on the analysis of multi-satellite systems and the consolidation of narrowband channel models. The availability of existing satellite constellations permitted performing on-field propagation experiments. Two major measurement campaigns were carried out, one in the US using the S-DARS satellites from XM Sirius satellites and another one in Europe using GPS satellites. Results on data analysis and a preliminary model development have been performed.

## I. INTRODUCTION

This paper describes the activities performed during the MiLADY project [1] including preparation and implementation of experiments, data analysis, modeling and results. The MiLADY project was carried out under contract of the European Space Agency in the frame of the ARTES-5 programme.

## II. EXISTING LMS CHANNEL MODELS FOR ANGLE DIVERSITY

Satellite broadcast to mobile services are subject to signal fades due to multipath, shadowing and blockage which strongly depend on the user environment. With new powerful satellites, even handheld applications with very small antennas become feasible. In particular, the US-based Digital Audio Radio Systems (DARS, known as Sirius XM Radio) have gained significant commercial importance. Future systems for distribution of digital media (audio / video) to portable and mobile receivers will require system architectures and link/physical layers that are able to overcome propagation effects on the land mobile satellite

(LMS) challenging environment. One of the typical mitigation techniques is based on diversity (time, space ...).

To achieve a good quality of service these systems already combine angle diversity technologies with time diversity/time interleaving. For mobile reception angle diversity may be combined with other technologies. It is therefore worthwhile to analyze the performance gain resulting from angle diversity together with time interleaving. For selected scenarios time interleaving may not be applicable. Therefore, performances gain with and without time interleaving needs to be evaluated.

The importance of an accurate modeling of the cross-correlation of angle diversity channels becomes obvious. For this cross-correlation, different approaches have been proposed in literature: some of them just assume totally uncorrelated channels, others are based on masking angle and masking functions derived from analysis of fish-eye cameras pictures, videos, or static circular measurements; there are others based on hybrid physical-statistical models, where the environment is generated from some statistical parameters and then physical propagation principles are applied on the synthetically generated environment. The case of masking functions represents shadowing only in a few discrete states (blocked, non-blocked, and sometimes shadowed state if vegetation can be distinguished from the pictures) giving as well discrete values of the cross-correlation, whereas the physical-statistical case, being in principle more realistic, depends on the accuracy and detail of the physical modeling and usually lacks validation from measurements. The objective of MiLADY was to perform measurement campaigns to gather relevant datasets to improve modeling and understanding of satellite angle diversity.

## III. MEASUREMENT CAMPAIGNS AND DATA PREPARATION

Two measurement campaigns were carried out within the MiLADY project:

- Satellite Digital Audio Radio Service (S-DARS) measurements in the United States relying on the two geostationary (GEO) satellites of XM Satellite Radio and three highly elliptical orbit (HEO) satellites of Sirius Satellite Radio (two in view at the same time)

This work has been published in the proceedings of the fourth IEEE European Conference on Antennas and Propagation (EuCAP), 2010

© 2010 IEEE. Personal use of this material is permitted. Permission from IEEE must be obtained for all other uses, in any current or future media, including reprinting /republishing this material for advertising or promotional purposes, creating new collective works, for resale or redistribution to servers or lists, or reuse of any copyrighted component of this work in other works

- Measurements in Europe using Global Positioning System (GPS) satellites in combination with a high accuracy GPS receiver.

The **first measurement campaign** was performed all along the US East Coast in September 2008. The route ranging from Jacksonville, Florida to Portland, Maine covered a total distance of 3700 km with 75 hours of measuring time (cf. Fig. 1). On the travelled route, a large variety of environments were passed. Power levels of 4 satellites in view were recorded simultaneously, each of them with different azimuth and elevation angles. A block diagram and a photo of the measurement setup are depicted in Fig. 2. For the purpose of documentation, two GPS receivers were active in the measurement van (Fig. 2): A front camera behind the windscreen and a fisheye camera on the van's rooftop covering the upper hemisphere. An additional wheel sensor allowed the accurate transformation of power level time series into a series with equidistant sampling as used in known channel models from literature [2], [5], [6].

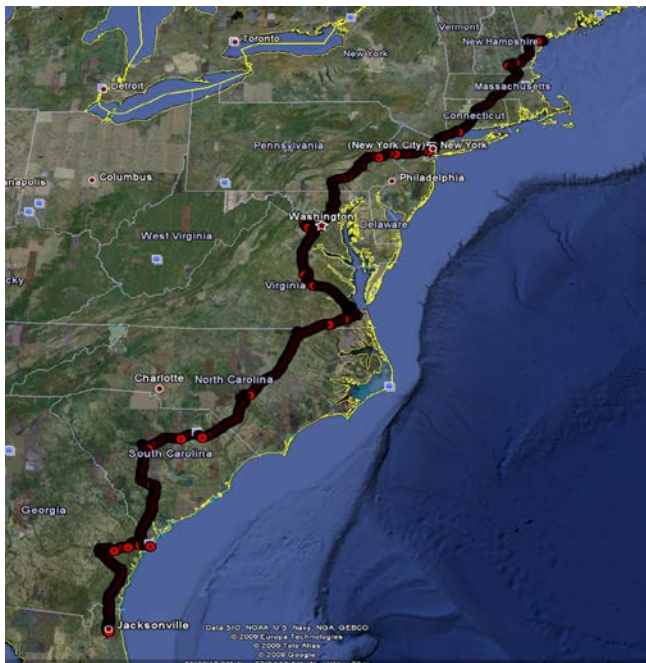


Fig. 1: Measurement route along US East Coast

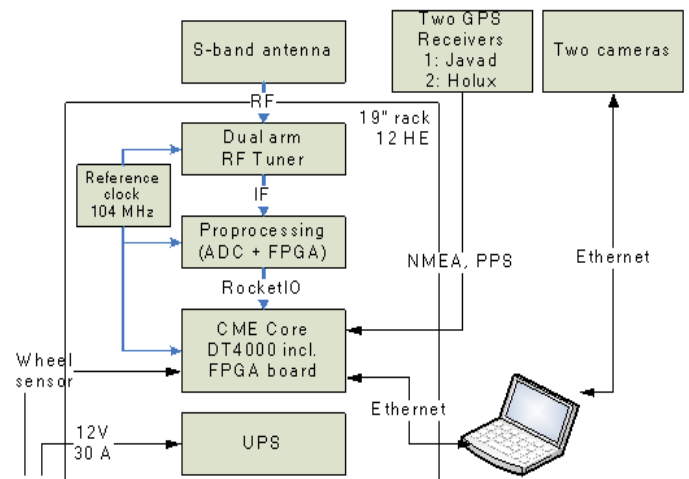


Fig. 2: Block diagram of measurement setup

The high sampling rate of the power levels (2.1 kHz) allowed analyzing the slow fading, as well as the fast fading effects of the propagation channel. Before that however, several pre-processing steps were performed:

- Splitting of the recorded measurement files in chunks with quasi constant elevation and azimuth angles. The elevations are in a range from  $23^\circ$  to  $83^\circ$ .
- Environment classification based on the front view and roof top camera data and subsequent splitting of measured power level data in several chunks with homogenous statistics (also called takes)
- Analysis of S-DARS satellites handovers and sections affected by interference from terrestrial SDARS repeaters.
- Calibration and line-of-sight normalization.

The **second measurement campaign** carried out in summer 2009 was based on GPS field trials in the area of Erlangen in Germany. Results are limited in the quantized resolution of 1 dB of received signal intensity C/N0 and in the sampling rate, which is 20 Hz. However, due to a high number of satellites in view (at least 8), many satellite orientations were analyzed to obtain slow fading characteristics (e.g. identification of LOS and shadowing/blocked state).

The measurement setup for the second campaign in Erlangen, Germany is based on the Javad professional GPS receiver, a device as already used during the US campaign. The receiver estimates the received C/N0 of the L1 carrier at 1575.42 MHz from each received GPS satellite signal. The overall dynamic range of the C/N0 estimation is around 20 dB.

A route of 38 km in the area of Erlangen comprising several environments such as urban, suburban and rural was chosen and driven 10 times to get a sufficient amount of orbit positions for the analysis of different possible angle diversity constellations. An overview on the azimuth and elevation angles is shown in Fig. 3.

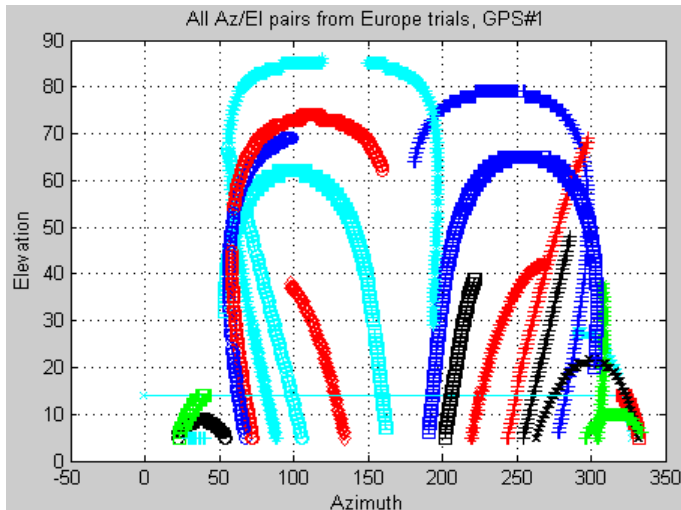


Fig. 3: Available azimuth and elevation angles of GPS satellite measurements in Erlangen.

#### IV. DATA ANALYSIS RESULTS

##### A. S-DARS Data Analysis

Data analysis was carried out both for single satellite and dual satellite scenarios by means of first and second order statistics.

The propagation characteristic of the mobile satellite reception depends strongly on the environmental features close to the receiver. Therefore, an accurate characterization of the environment is required. Using the image material from the two cameras, the entire database was derived into five different classes of environments: *urban*, *suburban*, *rural*, *commercial* and *highway*. An accurate description of the given environment types can be found in [4].

For studying the LMS channel characteristics of a single satellite a further division of the signals into different elevation ranges of  $10^\circ$  was made. The resulting measurement length depending on the environment classification and elevation of the satellites is summarized in table I.

TABLE I:

AVAILABLE MEASUREMENT LENGTH DEPENDING ON ENVIRONMENT AND ELEVATION

Length Environment	Elevation Angle				
	25°-35°	35°-45°	45°-55°	55°-65°	65°-75°
<b>Urban</b>	55 km	99 km	44 km	75 km	67 km
<b>Suburban</b>	79 km	141 km	93 km	116 km	117 km
<b>Rural</b>	139 km	513 km	582 km	427 km	191 km
<b>Highway</b>	1400km	1492km	1187km	1148km	1846km
<b>Commercial</b>	66 km	104 km	85 km	95 km	69 km

After clustering the recorded data into chunks with quasi equal receive conditions, first order statistics are derived from the carrier-to-noise ratio.

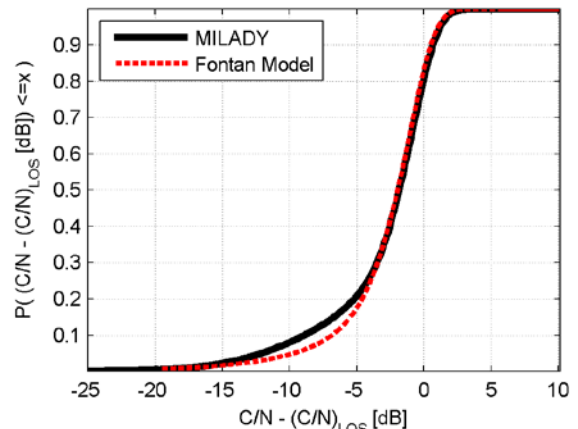


Fig. 4: Cumulative distribution function of the normalized carrier-to-noise signal in suburban environments and satellite elevation angles between  $35^\circ$  and  $45^\circ$  in comparison with the DVB-SH reference model ([2], [8]).

Fig. 4 shows the cumulative distribution functions (CDF) of the normalized carrier-to-noise signal in suburban environments and satellite elevation angles between  $35^\circ$  and  $45^\circ$ . 0 dB corresponds to the line-of-sight level (LOS level). The dashed line indicates the CDF of the suburban model for elevation angles of  $40^\circ$  as used for DVB-SH performance evaluation [8]. A deviation between the curves can be seen for fading deeper than 5 dB below the LOS level. This may result from differences in the measurement location: the parameters of the DVB-SH reference model are based on measurements in UK. The azimuth angle of reception there was mainly  $90^\circ$  to the driving direction. Nevertheless, the 'MiLADY'-signals represent environments as can be found in the USA, some of them are representative of a European case, and includes azimuth angles between  $0^\circ$  and  $360^\circ$ .

To characterize the environment, the required fade margin in order to provide specific signal availability can be extracted from the CDF. Assuming a signal availability of 90%, the required fade margin would be 9 dB for the 'MiLADY' database in the given example in Fig. 4. Detailed analysis results on this statistical parameter for the single satellite reception were already published in [3] and [4]. Required fade margins for the different environment classes and elevation ranges as shown in table I were analyzed for different lengths of time interleaving.

A first evaluation of angle diversity in dual satellite scenarios was made assuming maximum-ratio-combining (MRC) between the two signals. The resulting gain consists of a power combining gain (due to the increased overall signal because of a second satellite) and a diversity gain due to fading reduction.

Fig. 5 shows the CDFs of the normalized carrier-to-noise ratio of two single satellites 'XM Rock' and 'XM Roll' and the combined signal. The higher availability of 'XM Roll' is

because of an approx.  $15^\circ$  higher elevation than 'XM Rock' over the entire measurement route. From, Fig. 5 an MRC gain of 4 dB can be extracted for a signal availability of 90% related to the satellite with the higher elevation. Note that the average power of the MRC signal is increased by 3 dB in case of a simple signal power addition. If we compare the single satellite system with the dual satellite system, both with the same transmission power, then the diversity gain for a signal availability of 90% is 1 dB in this example (Fig. 5, dashed).

Analysis results for the dual satellite reception in terms of different environments and different interleaver lengths can be found in [4]. A detailed look on angle diversity effects due to different elevation angles and also due to the angular separation of the two satellites will be presented in further papers.

### B. GPS Data Analysis

The MILADY activity aimed also to provide a model able to represent most azimuth-elevation angle separation combinations and even several satellites from a constellation. For this assessment of the effect of angle diversity on the first and second order statistics of the received multi-satellite signal, GPS measurement data from the Erlangen trials with simultaneously at least 8 satellites in view were analyzed. The 10 measurement drives on the same route at different daytimes summarized to around 70 different pairs of azimuth and elevation angles for the same location. Consequently, there are around 2400 combinations of these 70 "virtual" satellites assuming a dual satellite scenario. Each combination is characterized by a pair of elevation angles and an azimuth separation which is introduced as simplification instead of pairs of azimuth angles.

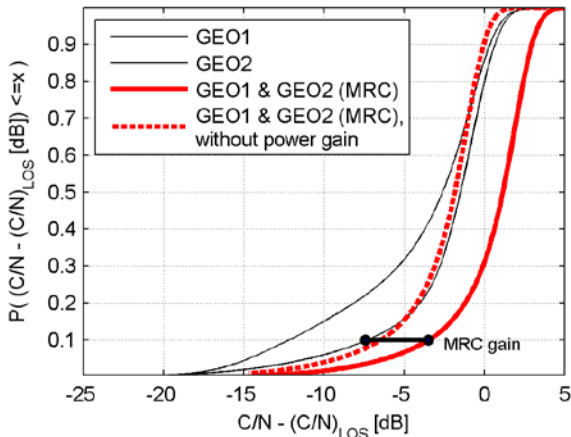


Fig. 5: Cumulative distribution functions of the normalized carrier-to-noise ratio of two geostationary satellites and of the Maximum-ratio-combined signal in suburban environments. The MRC gain for a signal availability of 90% is indicated. The dashed line results from the MRC of two half power satellites.

Dual satellite statistics have been obtained as follows. First, the estimated C/N0 values for both satellites were combined

assuming maximum ratio combining. Then, thresholds were placed. In case the signal is below the threshold the system is considered as unavailable (fading) otherwise as available. Several statistics have been computed of which only a limited set is presented here.

The share of samples affected by fades longer or equal than X is derived. It is either possible to fix a given X and determine the corresponding share of samples or the other way round. We decided to fix the share of samples affected by fades of length X to 1/100 and to determine the corresponding fade length X in samples. The results are presented in Fig. 6. This case investigates the impact of the azimuth separation in a rural environment, where both satellites had an elevation angle between  $30^\circ$  and  $40^\circ$ . As it is visible, the best results can be obtained for azimuth separation between  $50^\circ$  and  $150^\circ$ , what is not surprising. However, it should be also noted that azimuth separations of  $180^\circ$  may be also beneficial. Let's take the case of a road with trees on one side which block one satellite, but not its counterpart. Further investigation showed that by defining the correlation coefficient as the covariance between two discrete sample series with 0 for the signal being below a threshold and to 1 otherwise, a good match to Fig. 6 can be found. In other words, the fade length X can be approximated by the correlation coefficient. This is in particular interesting from the modeling point of view, since the knowledge of the correlation coefficient allows transforming two single satellite channel models into a dual satellite channel model [7].

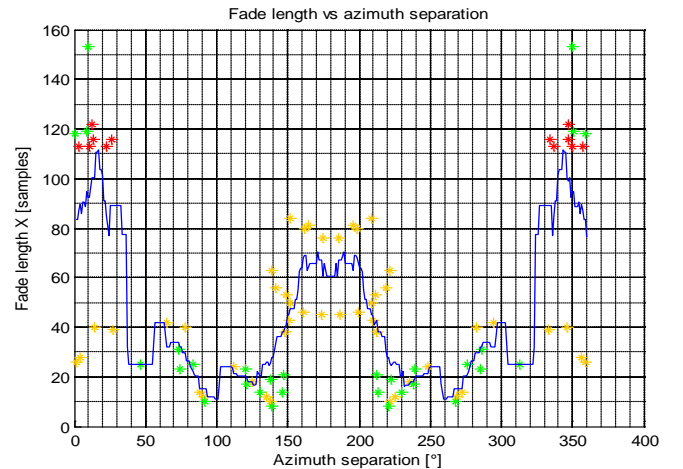


Fig. 6: Fade length vs. azimuth separation. In blue average over a sliding window of width  $20^\circ$ . In green satellites pairs in which both satellites lie in the upper half of the elevation range. In red satellite pairs in which both satellites lie in the lower half of the elevation range. All other satellite pairs are marked orange.

## V. PRELIMINARY CHANNEL MODEL

Following the baseline of existing reference LMS single satellite models, a Markov chain with three different states was used in order to describe slow fading events. The type of fast fading within the states was assumed to be Suzuki in blockage, Loo in shadowing and Rice in line-of-sight (LOS).

The probability density function of the power received 'x' in each state is:

- Blockage:  $f(x|S_0) = \frac{1}{S_0} e^{-\frac{x}{S_0}}$ , where  $S_0$  is the short term

mean power received, which follows a lognormal distribution with standard deviation  $\sigma_{suc}$  and mean  $\mu_{suc}$ .

- Shadowing:  $f(x|z) = c_{lo} e^{-c_{lo}(x+z^2)} I_0(2c_{lo}z\sqrt{x})$ , where  $c_{lo} = \frac{1}{2\sigma_{lo}^2}$  being  $2\sigma_{lo}^2$  the total power of the scattered

components and z is the short term amplitude of the line-of-sight component, which follows a lognormal distribution with standard deviation  $\sqrt{d_0}$  and mean  $\mu_{lo}$ .

- Line-of-sight:  $f(x) = c_{rice} e^{-c_{rice}(x+v_{rice}^2)} I_0(2c_{rice}v_{rice}\sqrt{x})$ , where  $c_{rice} = \frac{1}{2\sigma_{rice}^2}$  being  $2\sigma_{rice}^2$  the total power of the scattered

component and  $v_{rice}$  is the average amplitude of the line-of-sight component.

Table II provides the mean values of the parameters for all environments and elevation ranging from 30° to 50° (a subset of the total range of elevation angles). The parameters provided in the table are in accordance with well established models in [6] and [7].

For the multi-satellite modeling the state series of two out of the four available satellites for a given measurement route were combined. In order to reduce the parameter set required to describe the joint Markov chain a new modeling approach called master-slave concept was introduced. The master slave concept allows to take into account the correlation of the large scale fading effects in an efficient way and to compare the model parameter with single satellite models. Both satellites are described by conventional state based single satellite model and fast-fading can be simulated on top. However, the state transition probability matrix of the slave satellite changes with the state of the master satellite. This is because depending on the elevation and azimuth separation between the master and slave satellite, both can show similar, opposite or totally uncorrelated behavior. The conditional probability of the state transition of the slave satellite takes into account the correlation between the satellites. The master-slave concept allows also extending the model to more than two satellites.

## VI. CONCLUSIONS

The two measurement campaigns carried out within the MiLADY project allowed to build an extensive database of measurement data. The database has been used for a detailed link layer analysis and channel modeling of single and dual satellite systems for the special case of the S-DARS system in the US. Initial analysis of the correlation between different GPS satellite signals was performed with the purpose to extend the multi-satellite model to more generally distributed orbit positions.

Topic for future research is the extension of the current channel model. On one hand, the recorded GPS data allow to evaluate the correlation between satellites at various spatial separations, so the model can be extended to multi-satellite constellations. On the other hand, the introduction of adaptive state transition matrices will help to improve the accuracy of the model especially in urban environment.

Another subject of future work is to analyze antenna effects and the impact on the channel model parameters. Modeling the antenna effects helps to separate them from propagation effects.

## ACKNOWLEDGMENT

The MiLADY project partners wish to thank the European Space Agency for funding this activity.

## REFERENCES

- [1] MiLADY project web page: <http://telecom.esa.int/telecom/www/object/index.cfm?fobjectid=29200>
- [2] Perez-Fontan, F., Vazquez-Castro M, Enjamio Cabado, C., Pita Garcia, J. and Kubista, E., "Statistical Modelling of the LMS Channel", IEEE Trans. on Vehic. Techn., Vol. 50, No. 6, November 2001.
- [3] E. Eberlein, A. Heuberger, T. Heyn, "Channel models for systems with angle diversity – The MiLADY project", ESA Workshop on Radiowave Propagation Models, Tools and Data for Space Systems, ESTEC Noordwijk, the Netherlands, December 2008
- [4] D. Arndt, A. Ihlow, A. Heuberger, T. Heyn, E. Eberlein, "Land Mobile Satellite Channel Characteristics from the MiLADY Project", 10th workshop digital broadcasting, Ilmenau, Germany, September 2009
- [5] E. Lutz, D. Cygan, M. Dippold, F. Dolainsky, W. Papke. "The Land Mobile Satellite Communication Channel-Recording, Statistics and Channel Model", IEEE, Trans. On Vehic. Techn. Vol 40, No 2, May 1991.
- [6] C. Loo, "A Statistical Model for a land Mobile Satellite Link", IEEE Trans. On Vehic. Techn. Vol 34, August 1985
- [7] E. Lutz, "A Markov Model For Correlated Land Mobile Satellite Channels", International Journal of Satellite Communications, Vol. 14, p.p 333-339, 1996
- [8] DVB-SH implementation guidelines DVB bluebook A120 / dTS102584 (source: [http://www.dvb.org/technology/standards/a120.DVB-SH\\_implementation\\_guide.pdf](http://www.dvb.org/technology/standards/a120.DVB-SH_implementation_guide.pdf))

TABLE II:

MEAN FAST FADING PARAMETERS FOR ELEVATIONS BETWEEN 30° AND 50°. P(LOS), P(S), P(B) DENOTE THE PROBABILITY OF LINE-OF-SIGHT, SHADOWING AND BLOCKAGE STATE RESPECTIVELY.

Environment	Elevation	Line-of-sight			Shadowing				Blockage		
		P(LOS)	$C_{rice}$ (dB)	$v_{rice}$ (dB)	P(S)	$C_{loo}$ (dB)	$\mu_{loo}$ (dB)	$\sqrt{d_0}$ (dB)	P(B)	$\sigma_{suz}$ (dB)	$\mu_{suz}$ (dB)
Highway	30°	0.90	19.43	-0.13	0.07	8.6	-5.30	0.97	0.03	4.75	-9.22
	40°	0.89	19.04	-0.13	0.05	9.11	-3.8	0.78	0.06	7.15	-9.88
	50°	0.96	20.40	-0.01	0.01	3.86	-8.14	0.18	0.03	4.88	-9.73
Rural	30°	0.59	18.00	-0.17	0.21	11.21	-3.18	0.57	0.21	3.46	-7.61
	40°	0.78	17.49	-0.11	0.14	10.06	-2.77	0.85	0.09	3.12	-8.82
	50°	0.97	20.93	-0.23	0.02	9.01	-3.96	1.02	0.01	2.03	-7.38
Suburban	30°	0.66	15.70	-0.34	0.24	10.03	-3.59	0.84	0.10	3.20	-13.17
	40°	0.64	13.67	-0.39	0.30	9.25	-3.85	1.20	0.05	2.76	-10.61
	50°	0.71	16.14	-0.20	0.21	10.64	-2.72	0.86	0.08	3.61	-13.42
Urban	30°	0.23	13.38	-0.32	0.38	10.43	-3.25	2.99	0.38	2.39	-13.46
	40°	0.44	14.49	-0.28	0.47	7.85	-4.79	1.48	0.09	3.95	-13.44
	50°	0.54	14.87	-0.01	0.38	5.43	-5.30	1.96	0.07	4.28	-11.18